



## TECHNIQUE FOR MEASURING MAGNITUDES AND PHASES OF VOLTAGE AND CURRENT IN BAND-SELECTIVE PARALLEL LCR CIRCUIT

Hari Prasad Lamichhane\*

Central Department of Physics, Tribhuvan University, Kirtipur, Kathmandu, Nepal

\*Corresponding author: [hlamichhane1@gmail.com](mailto:hlamichhane1@gmail.com)

(Received: March 13, 2019; Revised: June 19, 2019; Re-revised: November 25, 2019; Accepted: November 26, 2019)

### ABSTRACT

The current in the parallel LCR (inductor, capacitor and resistor) circuit depends not only on the magnitude of the applied electromotive force (emf) but also on its frequency. The circuit current in the parallel LCR circuit becomes very small in the resonating region, but at the same time, the potential difference across the LC tank becomes very large. These results are justified if there is a large induced current in the LC tank in such a way that the inductive and capacitive branch currents are nearly out of phase so that the vector sum of the currents be minimal. This theory can be verified by inserting a small series resistor in each branch. Finally, calculated magnitudes and phases of the potential differences across the newly connected resistors which are directly related to the magnitudes and phases of corresponding branch currents verify the theory.

**Keywords:** LCR circuit, Internal tank current, Phase difference, Antiresonance, Sensitivity

### INTRODUCTION

An inductor, capacitor and resistor (LCR) circuit are essential for studying resonance phenomena. The resonating LCR circuits have a wide range of applications in designing various electronic devices (Amin *et al.*, 2018; Teymour *et al.*, 2014; Pan *et al.*, 2015; Choi *et al.*, 2015; Li & Xu, 2014; Li *et al.*, 2012; Buccella *et al.*, 2017). Both inductive reactance and capacitive reactance depend on the frequency of the ac source. The magnitude of the inductive reactance is directly proportional to the frequency, whereas, the extent of capacitive reactance is inversely proportional to the frequency (Ryder, 2012; Pipes & Harvill, 1971; Halliday *et al.*, 2001; Reitz *et al.*, 1998).

Besides, the inductive reactance induces  $90^\circ$  phase difference between the voltage and the current, but the capacitive reactance induces  $-90^\circ$  phase difference between the voltage and the current (Ryder, 2012). As the frequency of the ac source gradually increases from a small value or decreases from a significant amount, the inductive reactance and capacitive reactance become equal in magnitude and opposite in sign at a particular frequency. At this frequency, called resonant frequency, these two reactances cancel each other in the series LCR circuit, and the circuit impedance becomes minimum, and thus, maximum source current flows in the circuit.

On the other hand, the source current becomes minimum or impedance becomes maximum at resonance condition in the parallel LCR circuit (Fig. 1). Since the inductor is in series to the capacitor within the LC tank loop, it induces a maximum internal current in the LC tank at the resonant frequency. The external ac source only supplies power to the LC tank equal to the power loss in the total resistance

in the LC tank (Ryder, 2012). In the ideal condition, the LC tank resistance is zero, and there is no loss of power in the LC tank, and the induced current sustains forever without the external ac source supplying additional power to the LC tank. That is why the source current becomes the smallest at resonance condition (also called anti-resonance condition) in the parallel LCR circuit (Ryder, 2012).

This fact can be verified by measuring magnitudes and phase of currents and potential differences by inserting small resistors in both branches. While ascertaining the theory, the effect of additional resistors will be compared with the ideal values by using Excel-2010 program. This article will be useful for analyzing the results of a parallel LCR circuit experiment in Physics Master's degree course at different universities of Nepal.

### MATERIALS AND METHODS

#### a) Calculation of admittance, impedance, currents and anti-resonance frequency when a resistor is present in the L-branch

The inductor is generally made from winding a conducting wire. Because of finite resistivity of the wire material, small cross-sectional area and long length, the inductor has some resistance. The effect of the coil resistance comes in series to the inductance of the coil in the equivalent circuit (Ryder, 2012). A parallel LCR circuit with a resistor in the L-branch and a sinusoidal voltage  $V_s$  sets up a sinusoidal current  $I$  in the circuit, as shown in Fig. 1. The source current  $I_1$  is divided into  $I_L$  and  $I_C$  in the tank. The inductive ( $I_L$ ) and the capacitive ( $I_C$ ) currents can be expressed in terms of LC tank voltage  $V_0$  and corresponding admittances as,  $I_L = Y_L V_0$  and  $I_C = Y_C V_0$ .

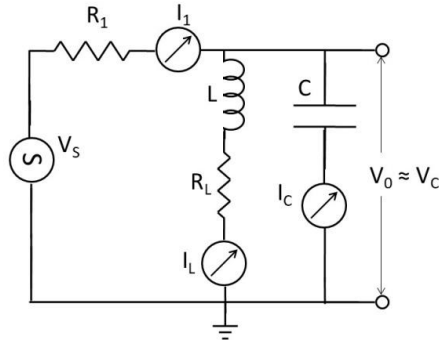


**Fig. 1. Parallel LCR circuit** (Ryder, 2012)

By neglecting the impedance of the current meter, the admittance of the tank circuit can be calculated as given in equation (1) (Ryder, 2012; Pipes & Harvill, 1971; Halliday *et al.*, 2001; Reitz *et al.*, 1998).

$$Y_0 = Y_L + Y_C = \frac{1}{R_L + j\omega L} + j\omega C = \frac{R_L}{R_L^2 + \omega^2 L^2} + j\left(\omega C - \frac{\omega L}{R_L^2 + \omega^2 L^2}\right) \quad (1)$$

The anti-resonance condition of the circuit is obtained when the imaginary part of the admittance is equal to zero. Therefore, the anti-resonance frequency

$$f_{ar} = \frac{\omega_{ar}}{2\pi} = \frac{1}{2\pi} \sqrt{\frac{1}{LC} - \frac{R_L^2}{L^2}} \quad (2)$$

The impedance of the tank circuit at the anti-resonance condition is:

$$Z_{ar} = \frac{R_L^2 + \omega_{ar}^2 L^2}{R_L} = \frac{L}{CR_L} \quad (3)$$

### Sensitivity

Parallel LCR circuit is usually used for selecting a particular signal from a mixture. For example, tuning a radio signal means separating the right signal from a combination of many radio waves (Comer & Comer, 2003). The sensitivity of parallel LCR circuit depends not only on the impedance of the tank circuit but also on the value of the series resistance  $R_1$ . The sensitivity of parallel LCR circuit increases with an increase in the value of  $R_1$ . The sensitivity ( $S$ ) of a resonating circuit can be defined as:  $S = \frac{f_0}{f_2 - f_1}$  (4)

The frequencies  $f_0$ ,  $f_1$  and  $f_2$  are the values of frequencies corresponding to the maximum value of the LC tank voltage ( $V_{0max}$ ) and lower and upper half power points where  $V_0 = 0.707 V_{0max}$ .

### b) Calculation of admittance, currents and anti-resonance frequency when resistors are present in both branches

Magnitudes of the inductive and capacitive currents can be measured by using an ac current meter. However, their

relative phase is still unknown. Additional small resistors can be added in series in both branches to measure voltages with the help of an oscilloscope. Parallel LCR circuit with resistors in both branches is shown in Fig. 2.

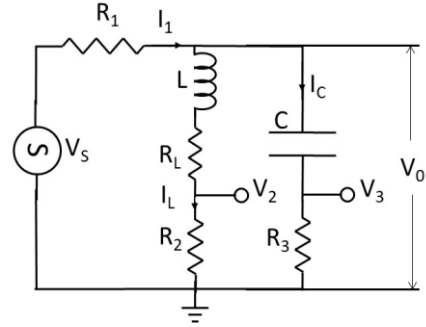


**Fig. 2. Parallel LCR circuit with resistances present in both branches** (Ryder, 2012)

Although the position of anti-resonance frequency slightly changes with the inclusion of resistances in both branches, this circuit is still useful to find out relative phases of currents through the inductor and the capacitor in the parallel LCR circuit. Since the current and voltage are in phase in the resistor, the phase difference between  $V_2$  and  $V_3$  in the circuit shown in Fig. 2 is also the phase difference between  $I_L$  and  $I_C$ . After measuring magnitudes and relative phase of  $V_2$  and  $V_3$  using a dual-channel oscilloscope, one can calculate the magnitudes of currents as;  $I_L = V_2/R_2$  and  $I_C = V_3/R_3$ . (5)

Also, the relative phase of  $I_L$  and  $I_C$  is equal to the relative phase of  $V_2$  and  $V_3$ .

The admittance of the tank circuit, as shown in Fig. 3 can be calculated to be

$$Y_0 = Y_L + Y_C = \frac{1}{R_L + R_2 + j\omega L} + \frac{1}{R_3 - \frac{j}{\omega C}} \quad (6)$$

The admittance and the LC tank voltage ( $V_0$ ) can be used to calculate currents as:

$$I_L = Y_L V_0 = \frac{1}{R_L + R_2 + j\omega L} V_0 = \left[ \frac{R_L + R_2}{(R_L + R_2)^2 + \omega^2 L^2} - j \frac{\omega L}{(R_L + R_2)^2 + \omega^2 L^2} \right] V_0 \quad (7)$$

and,

$$I_C = Y_C V_0 = \frac{1}{R_3 - \frac{j}{\omega C}} V_0 = \left[ \frac{R_3}{R_3^2 + \frac{1}{\omega^2 C^2}} + j \frac{\frac{1}{\omega C}}{R_3^2 + \frac{1}{\omega^2 C^2}} \right] V_0 \quad (8)$$

as well as

$$I_1 = Y_0 V_0 = \left\{ \left[ \frac{R_L + R_2}{(R_L + R_2)^2 + \omega^2 L^2} + \frac{R_3}{R_3^2 + \frac{1}{\omega^2 C^2}} \right] + j \left[ \frac{\frac{1}{\omega C}}{R_3^2 + \frac{1}{\omega^2 C^2}} - \frac{\omega L}{(R_L + R_2)^2 + \omega^2 L^2} \right] \right\} V_0 \quad (9)$$

Finally, the source voltage can be expressed in terms of tank voltage as

$$V_0 = \frac{V_s}{1 + Y_0 R_1} \quad (10)$$

An imaginary number can be expressed in terms of magnitude ( $r$ ) and phase angle ( $\theta$ ) as (Ryder, 2012; Pipes & Harvill, 1971; Halliday *et al.*, 2001)

$$z = x + jy = r e^{j\theta} \quad (11)$$

Where,  $r = \sqrt{x^2 + y^2}$  and  $\theta = \tan^{-1} \left( \frac{y}{x} \right)$  (12)

Anti-resonance frequency of parallel LCR circuit with resistances present in both branches can be calculated to be (Ryder, 2012)

$$f_{ar} = \frac{1}{2\pi} \sqrt{\frac{1}{LC} \left( \frac{L - R_0^2 C}{L - R_3^2 C} \right)} \quad (13)$$

Where,  $R_0 = R_L + R_2$ .

The circuit shown in Fig. 2 reduces to the circuit shown in Fig. 1 when resistors  $R_2$  and  $R_3$  become zero. If the values of  $R_2$  and  $R_3$  are minimal compared to the magnitudes of inductive and capacitive reactance, the phase difference between  $V_2$  and  $V_3$  can approximately be taken as the phase difference between the currents flowing through the inductive and the capacitive branches in the absence of  $R_2$  and  $R_3$ . Excel-10 program was used to compute current and voltage and to plot their graphs. Power point is used to construct circuit diagrams and figures.

### RESULTS AND DISCUSSION

One can theoretically extract some important results related to the current and voltage of the parallel LCR circuit by selecting component values. The component values were chosen as: a variable frequency sinusoidal source voltage ( $V_s$ ) = 5 V peak; Inductor,  $L = 50$  mH, coil resistance ( $R_L$ ) = 100  $\Omega$ ; Capacitor,  $C = 0.01 \mu\text{F}$  and resistors  $R_1 = 5$  k $\Omega$ ,  $R_2 = 50 \Omega$  and  $R_3 = 50 \Omega$ . The experimental circuit is shown in Fig. 3.

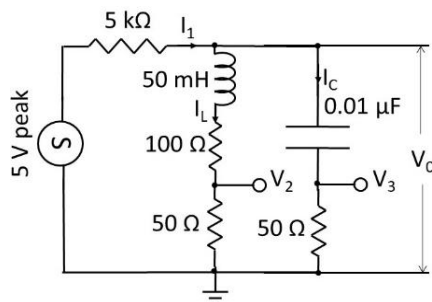


**Fig. 3. An example of the experimental circuit for measuring relative phases of inductor and capacitor currents**

### a) Calculation of potential difference across the LC tank ( $V_0$ )

A graph of the calculated values of the potential difference across the LC tank (output voltage) by varying the signal frequency and keeping input voltage constant is plotted in Fig. 4. Whenever the series resistance  $R_1$  is zero, the output voltage is always equal to the source voltage. Thus, a parallel LCR circuit with zero series resistance will be indifferent to all frequencies, and hence its sensitivity should be equal to zero. On the other hand, the output voltage monotonically increases from zero to a maximum value 4.55 V as the frequency increases from zero to 7188 Hz for the input voltage 5 V and then gradually decreases when the frequency further increases in the presence of 5 k $\Omega$  series resistance  $R_1$ . This output voltage plot has a half-power frequency width of 3502 Hz.

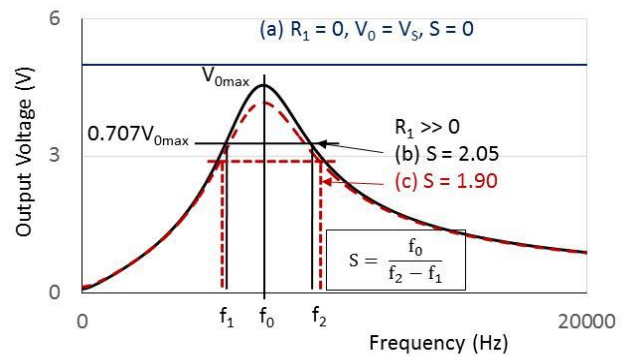


**Fig. 4. Dependence of the magnitude of the output potential difference ( $V_0$ ) across the LC tank circuit shown in Fig. 2 with  $V_s = 5$  V,  $L = 50$  mH,  $C = 0.01 \mu\text{F}$ ,  $R_L = 100 \Omega$  on the frequency of the applied sinusoidal voltage for a)  $R_1 = 0 \Omega$ , b)  $R_1 = 5$  k $\Omega$ ,  $R_2 = R_3 = 0 \Omega$  and c)  $R_1 = 5$  k $\Omega$ ,  $R_2 = R_3 = 50 \Omega$**

As a measure of the sharpness of resonance, the calculated sensitivity (equation 4) of the circuit without additional resistors  $R_2$  and  $R_3$  was found to be 2.05. As observed in Fig. 4, the height of the output voltage and frequency width at half power frequency also depended on the additional resistors  $R_2$  and  $R_3$  (Fig. 2). By the inclusion of 50  $\Omega$  resistors  $R_2$  and  $R_3$ , the height, position and frequency width of the output voltage plot for an input 5 V signal respectively became 4.17 V, 7186 Hz, and 3788 Hz. Hence, the sensitivity of the circuit slightly decreased to 1.90 upon inclusion  $R_2$  and  $R_3$ . Surprisingly, at the maximum output voltage position, the  $V_0$  was somewhat lagging in phase with the  $V_s$  when  $R_1$  was different from zero.

Relative magnitudes and phases of voltages across the source ( $V_s$ ) and the LC tank ( $V_0$ ) in the circuit is shown in Fig. 3 at the frequencies a) 7103 Hz, b) 3552 Hz and c) 14206 Hz are graphically shown in Fig. 5 and the corresponding values are given in Table 1. The potential difference across the LC tank ( $V_0$ ) is almost equal in

magnitude to the source voltage,  $V_S$  at 7103 Hz, the resonant frequency.  $V_0$  and  $V_S$  are in phase at the resonant frequency (Fig. 5a). At 3552 Hz, half of the resonant frequency, the output voltage reduces to slightly less than the one-third value of output voltage at the resonance frequency (Fig. 5b). The output voltage also leads the source voltage by  $65.1^\circ$ , thus reflecting the inductive nature of the output tank at a lower frequency. On the other hand, at 14206 Hz, the output voltage was slightly greater than one-third of the output voltage at resonant frequency (Fig. 5c). The output voltage was lagging in phase with the source voltage by  $69.7^\circ$ . This result clearly indicates the capacitive nature of output voltage at a higher frequency.

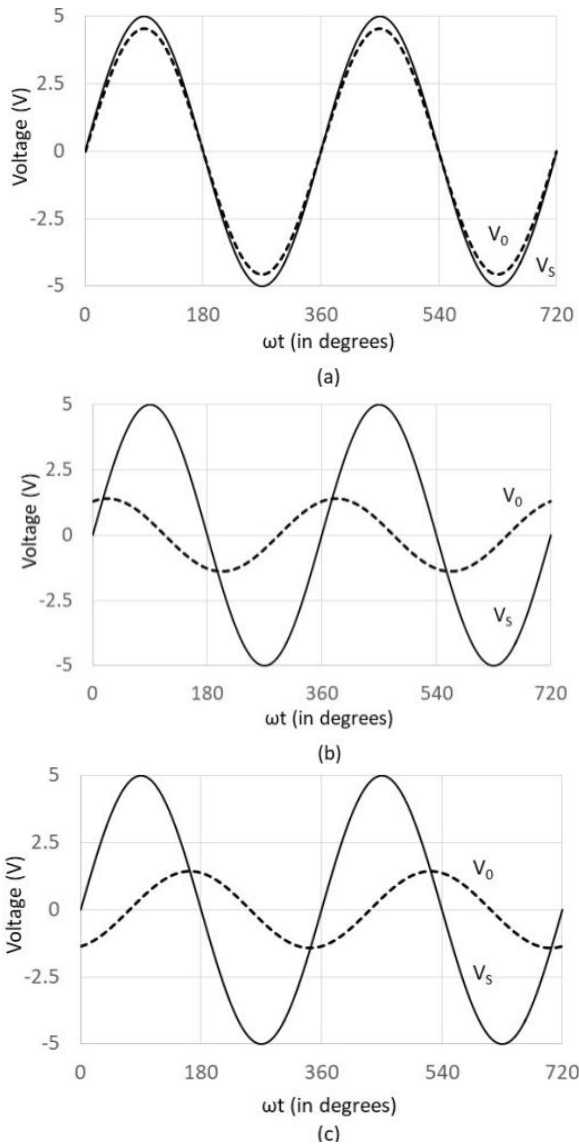


**Fig. 5. Relative magnitudes and phases of voltages across the source ( $V_S$ ) and LC tank ( $V_0$ ) in the typical experimental circuit shown in Fig. 3 at the frequencies (a) 7103 Hz, (b) 3552 Hz & (c) 14206 Hz**

**Table 1. Calculated values of LC tank voltage ( $V_0$ ) and relative phase ( $\phi$ ) between  $V_0$  and  $V_S$  at three set of frequencies in the circuit shown in Fig. 3**

Frequency	LC tank voltage, $V_0$	Phase angle ( $\phi$ ) between $V_0$ & $V_S$
7103 Hz	4.17 V	$0.0^\circ$
3552 Hz	1.26 V	$65.1^\circ$
14206 Hz	1.41 V	$-69.7^\circ$

**b) Calculated values of source current ( $I_1$ ), inductor current ( $I_L$ ) and capacitor current ( $I_C$ )**

Computed values of source current ( $I_1$ ), inductor current ( $I_L$ ) and capacitor current ( $I_C$ ) as a function of frequency using experimental circuit (Fig. 3) are shown in Fig. 6. The maxima/minima values of the currents are tabulated in Table 2.

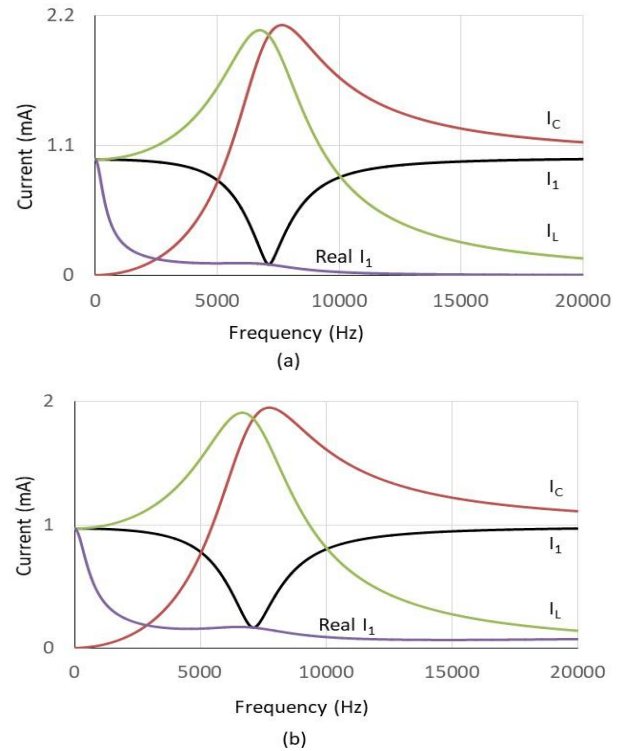


**Fig. 6. Computed graph between currents and frequency with  $V_S = 5$  V,  $L = 50$  mH,  $C = 0.01$   $\mu$ F,  $R_1 = 5$  k $\Omega$  and  $R_L = 100$   $\Omega$  using circuit shown in Fig. 2 when (a)  $R_2 = R_3 = 0$   $\Omega$  and (b)  $R_2 = R_3 = 50$   $\Omega$**

As can be seen that even with the addition of  $R_2 = R_3 = 50$   $\Omega$  in the circuit, the nature of the dependence of capacitor and inductor currents on the frequency does not alter. Magnitudes of capacitor and inductor currents slightly decreased, whereas the source current slightly increased. Maxima position of the capacitor current increased by 87 Hz and maxima position of the inductor current decreased

by 78 Hz with the addition of 50 Ω resistors in both branches. The minimum position of the source current is also decreased by 8 Hz. The source current was equal to its real value at its minima position.

**c) Relative magnitudes and phase differences among  $I_1$ ,  $I_L$  and  $I_C$**

Magnitudes and phase difference between the inductor current and capacitor current in the LC tank circuit can be

obtained using the circuit shown in Fig. 3. From the experimentally measured values of magnitudes and phase differences of potential differences  $V_2$  and  $V_3$  using an oscilloscope and equation 5 corresponding magnitudes and phases of currents can be extracted. Time dependence of currents at the resonant frequency ( $f_0$ ) and also at frequencies  $f_0/2$  and  $2f_0$  are shown in Fig. 7 and their numerical values are summarized in Table 3.

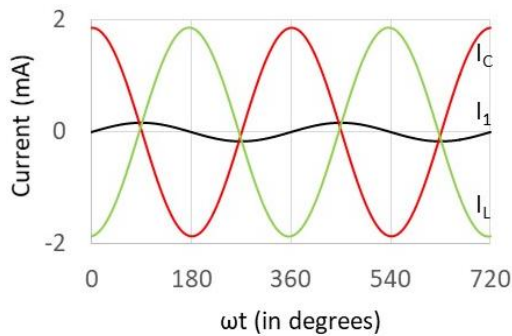
**Table 2. Extreme values and positions of currents in the circuit shown in Fig. 4**

Currents	Magnitude and position of currents for $R_2= R_3= 0 \Omega$		Magnitude and position of currents for $R_2= R_3= 50 \Omega$	
	Magnitude	Frequency	Magnitude	Frequency
$I_C$	2.119 mA	7656 Hz	1.952 mA	7743 Hz
$I_L$	2.075 mA	6749 Hz	1.911 mA	6671 Hz
$I_1$	0.091 mA	7111 Hz	0.166 mA	7103 Hz
$I_1$ Real	0.091 mA	7111 Hz	0.166 mA	7103 Hz

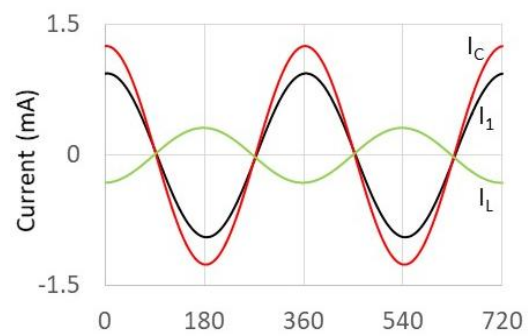
**Table 3. Calculated amplitudes of  $I_C$ ,  $I_L$  and  $I_1$  currents and their relative phases ( $\phi$ ) with respect to  $V_0$  at three sets of frequency using the circuit shown in Fig. 3**

Frequency	$I_1$ (mA)	$I_C$ (mA)	$I_L$ (mA)	$\phi_C$	$\phi_L$	$\phi_C-\phi_L$	$\phi_{I1}$
7103 Hz	0.17	1.86	1.86	88.7°	-86.2°	174.9°	-0.1°*
3552 Hz	0.91	0.31	1.22	89.4°	-82.3°	171.7°	-79.6°
14206 Hz	0.94	1.25	0.32	87.4°	-88.1°	175.5°	85.9°

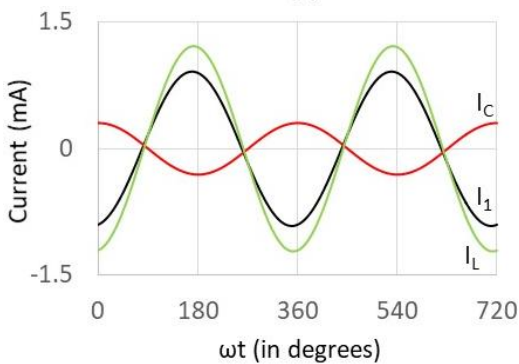
\*zero phase difference position lies in the frequencies between 7103 Hz and 7104 Hz



(a)



(c)



(b)

**Fig. 7. Calculated values of currents in the circuit shown in Fig. 3 at the frequencies (a) 7103 Hz, (b) 3552 Hz and (c) 14206 Hz**

Figure 7 and Table 3 show that inductor current was almost 180° out of phase to the capacitor current. The inductor and capacitor currents in the circuit 3 were equal in magnitudes at 7103 Hz, the resonant frequency. The source current was much smaller than either current at this frequency and was in phase with the output voltage. The source current leads the inductor current and lag capacitor current by nearly 90° each. However, at the half of the

resonant frequency, the capacitor current becomes smaller, and the inductor current dominates the source current. On the other hand, the source current was governed by the capacitor current at double of the resonant frequency.

## CONCLUSION

The magnitude and phase relationships of the inductor and capacitor currents in the band selective LCR parallel circuit can be measured by inserting small resistors in both branches. Although the presence of extra small resistors in the inductive and the capacitive branches somewhat alters the magnitudes of the currents, the nature of currents does not change much.

The output voltage across the LC tank circuit becomes maximum and comes in phase with the source voltage at the resonance. The output voltage leads/lags the source voltage at lower/higher frequencies. The inductor current is almost  $180^\circ$  out of phase with the capacitor current in the LC tank circuit. This result suggests that the most of inductor and capacitor currents are circulating in the LC tank. As the source current is the vector sum of inductor and capacitor currents, the source current becomes smallest at the resonance because the inductor and capacitor currents are almost equal and  $180^\circ$  out of phase, thus, resulting in maximum circulating current in the LC tank circuit.

## ACKNOWLEDGEMENT

I am grateful to Mr. Tika Ram Lamichhane and Mr. Rabindra Raj Oliya for their academic and technical help.

## REFERENCES

- Amin, M., Ramzan, R., & Siddiqui, O. (2018). Slow wave applications of electromagnetically induced transparency in microstrip resonator. *Scientific Reports*, 8, 2357-2361.
- Buccella, C., Cecati, C., Cimatorini, M. G., Kulothungan, G., Edpuganti, A., & Rathore, A. K. (2017). A selective harmonic elimination method for five-level converters for distributed generation. *IEEE Transactions on Power Electron*, 5(2), 775-783.
- Choi, U. M., Blaabjerg, F., & Lee, K. B. (2015). Reliability improvement of a T-type three-level inverter with fault-tolerant control strategy. *IEEE Transactions on Power Electronics*, 30(5), 2660-2673.
- Comer, D. J., & Comer C. T., (2003). *Advanced electronic circuit design*. New York, USA: John Wiley & Sons.
- Halliday, D., Resnick, R., & Walker, J. (2001). *Fundamentals of physics* (6<sup>th</sup> ed.). New York, USA: John Wiley & Sons.
- Li, R., & Xu, D. (2014). A zero-voltage switching three-phase inverter. *IEEE Transactions on Power Electron*, 27, 1200-1210.
- Li, R., Ma, Z., & Xu, D. (2012). A ZVS grid-connected three-phase inverter. *IEEE Transactions on Power Electronics*, 27(8), 3595-3604.
- Pan, D., Ruan, X., Bao, C., Li, W., & Wang, X. (2015). Optimized controller design for LCL L-type grid-connected inverter to achieve high robustness against grid-impedance variation. *IEEE Transactions on Industrial Electronics*, 62(3), 1537-1547.
- Pipes, L. A., & Harvill, L. R. (1971). *Applied mathematics for engineers and physicists*. Singapore: TaTa McGraw-Hill.
- Reitz, J. R., Milford, F. J., & Christy, R. W. (1998). *Foundations of electromagnetic theory*. New Delhi, India: Narosa Publishing House.
- Ryder, J. D. (2012). *Networks, lines ad fields*. New Delhi, India: PHI Learning Private Limited.
- Teymour, H. R., Sutanto, D., Muttaqi, K. M., & Ciufu, P. (2014). Solar PV and battery storage integration using a new configuration of a three-level NPC inverter with advanced control strategy. *IEEE Transactions on Energy Conversion*, 29(2), 354-365.